The American Journal of Pathology, Vol. 182, No. 2, February 2013

The American Journal of PATHOLOGY

ajp.amjpathol.org

VASCULAR BIOLOGY, ATHEROSCLEROSIS, AND ENDOTHELIUM BIOLOGY

Apoptosis Signal—Regulating Kinase 1 Deficiency Attenuates Vascular Injury—Induced Neointimal Hyperplasia by Suppressing Apoptosis in Smooth Muscle Cells

Takashi Tasaki,* Sohsuke Yamada,* Xin Guo,* Akihide Tanimoto,*† Ke-Yong Wang,* Atsunori Nabeshima,* Shohei Kitada,*‡ Hirotsugu Noguchi,* Satoshi Kimura,* Shohei Shimajiri,* Kimitoshi Kohno,§ Hidenori Ichijo,¶ and Yasuyuki Sasaguri*

From the Departments of Pathology and Cell Biology, Urology,‡ and Molecular Biology,§ School of Medicine, University of Occupational and Environmental Health, Kitakyushu; the Department of Molecular and Cellular Pathology,† Kagoshima University Graduate School of Medical and Dental Sciences, Kagoshima; and the Laboratory of Cell Signaling,¶ Graduate School of Pharmaceutical Sciences, The University of Tokyo, and Core Research for Evolutional Science and Technology, Tokyo, Japan*

Accepted for publication October 19, 2012.

Address correspondence to Sohsuke Yamada, M.D., Ph.D., Department of Pathology and Cell Biology, School of Medicine, University of Occupational and Environmental Health, 1-1 Iseigaoka, Yahatanishi-ku, Kitakyushu 807-8555, Japan. E-mail: sousuke@med.uoeh-u.ac.jp.

Apoptosis signal—regulating kinase 1 (ASK1) is a mitogen-activated protein kinase kinase kinase that plays a crucial role in stress-induced apoptosis. Recently, we have reported that suppressed macrophage apoptosis in ASK1 and apolipoprotein E double-knockout mice accelerates atheromatous plaques in the hyperlipidemia-induced atherosclerotic model. However, the pathogenic role of smooth muscle cell (SMC) apoptosis in atherosclerosis still remains unclear. We investigated neointimal remodeling in ligated carotid arteries of *ASK1*-deficient mice (*ASK1*$^{-/-}$) for 3 weeks. *ASK1*$^{-/-}$ mice had significantly more suppressed intimal formation, inversely manifesting as potential anti-atherogenic aspects of *ASK1* deficiency, characterized by fewer SMCs and less collagen synthesis; and fewer apoptotic SMCs, infiltrating T lymphocytes, and microvessels, associated with decreased apoptosis of luminal endothelial cells, compared with those of wild-type mice. Injured arteries of *ASK1*$^{-/-}$ mice also showed significantly down-regulated expression of pro-apoptotic markers, adhesion molecules, and pro-inflammatory signaling factors. Moreover, tumor necrosis factor-α—induced apoptosis was markedly suppressed in cultured aortic SMCs from *ASK1*$^{-/-}$ mice. These findings suggest that ASK1 accelerates mechanical injury—induced vascular remodeling with activated SMC migration via increased neovascularization and/or enhanced SMC and endothelial cell apoptosis. ASK1 expression, especially in the SMCs, might be crucial, and reciprocally responsible for various pro-atherogenic functions, and SMC apoptosis seems to be detrimental in this model. *(Am J Pathol 2013, 182: 597—609; http://dx.doi.org/10.1016/j.ajpath.2012.10.008)*

Investigations of arterial reaction against altered blood flow or mechanical injury offer potential clues for human atherosclerosis etiology and restenosis, a major cause of morbidity in humans.[1,2] *In vivo* atherosclerotic vascular lesions and remodeling, induced by unilateral carotid artery ligation and predominantly composed of migrating and/or replicating vascular smooth muscle cells (SMCs), with subsequent production of extracellular matrix, have been used as an injury model.[3] In this model, partial blood stasis, enhanced wall tension, and reduced shear stress induce vascular remodeling proximal to the ligature site, similar to atherosclerosis or restenosis after angioplasty.[2–5]

Apoptotic cells, including SMCs, endothelial cells (ECs), and macrophages, are reportedly evident in atherosclerosis.[6,7] Although there are few reports correlating SMC apoptosis with neointimal vascular remodeling in ligation-mediated atherosclerotic models, apoptosis of medial SMCs might accelerate injury-induced neointimal formation, probably by triggering migration and proliferation of SMCs.[8] On the other

Supported in part by Grants-in-Aid for Scientific Research (19590413, 20590416, and 24790394) from the Ministry of Education, Culture, Sports, Science and Technology, Tokyo, Japan (S.Y., A.T., and Y.S.).

T.T. and S.Y. contributed equally to this work.

http://dx.doi.org/10.1016/j.ajpath.2012.10.008

hand, apoptotic intimal SMCs are often not scavenged because of weakened phagocytic clearance (ie, efferocytosis) by macrophages; therefore, they could be the source of extracellular matrix, such as collagen and calcifying vesicles, or thrombin, resulting in the intimal thickening, calcification, or thrombogenicity, respectively.[9,10] Apoptosis of ECs could also be important in the ligation model, because the initial step for injury-induced atherosclerosis includes EC damage and subsequent inflammatory cell migration.[6,11] Despite this, the role of apoptosis by vascular SMCs and/or ECs in the progression of neointimal hyperplasia is still debatable; apoptosis might also be a part of normal vascular wound healing.[12]

Apoptosis signal–regulating kinase 1 (ASK1), which is a mitogen-activated protein kinase kinase kinase family member, is stimulated via distinct mechanisms in response to various cytotoxic stressors, such as oxidative stress mediated by hydrogen peroxide, endoplasmic reticulum stress, and immune system mediators, such as tumor necrosis factor (TNF), IL-1, or Fas ligands.[13,14] ASK1 activates the c-Jun N-terminal kinase and p38 mitogen-activated protein kinase signaling pathways, which subsequently induce intrinsic apoptosis through mitochondria-dependent caspase activation.[13–15] More recently, our research has shown that suppressed macrophage apoptosis in ASK1 and apolipoprotein E (apoE) double-knockout ($ASK1^{-/-}/apoE^{-/-}$) mice accelerates macrophage-rich atheromatous plaques, coincident with fewer necrotic cores in the hyperlipidemia-induced atherosclerotic model,[15] unlike in the current injury-induced neointimal remodeling. Reported data indicate that ASK1 signaling attenuates macrophage-rich atherosclerosis and enhances necrotic core formation by stimulating macrophage apoptosis, which might cause plaque vulnerability via necrotic core development. ASK1 plays a critical role in the regulation of macrophage apoptosis from the anti-atherogenic aspects.[15]

However, little is known about the relationship between apoptosis in ASK1-induced SMCs and/or ECs and vascular remodeling of atherosclerotic models. Actually, another group has reported ASK1 activation to play a key role in vascular neointimal hyperplasia[16]; however, their balloon injury model on rat carotid arteries is not suitable to examine EC apoptosis and, inconsistently, their data have not demonstrated that dominant-negative ASK1 mutant significantly decreases vascular SMC apoptosis. By contrast, we suggested that the mechanisms responsible for atherosclerosis in vascular injury–induced arteries would be fundamentally different from those at play in the high-cholesterol diet–induced aortas in rabbit models.[17] Thus, in the present study, we examined the roles of ASK1 and apoptosis of SMCs and/or ECs in ligation injury–induced neointimal hyperplasia.

Materials and Methods

Animals

The experiments were performed on young male C57BL/6 wild-type (WT) and $ASK1^{-/-}$ mice,[15] weighing 20 to 25 g. To produce the ligation-induced vascular injury model, we ligated the left common carotid artery with a 7-0 silk suture at a site proximal to the carotid bifurcation in two groups of mice at the age of 6 to 8 weeks under anesthesia: an i.p. injection of 100 mg/kg ketamine (Daiichi Sankyo Co, Tokyo, Japan) and 2 mg/kg medetomidine (Meiji Yakuhin Co, Tokyo). The animals were euthanized at 1, 2, or 3 weeks after injection, by an i.p. injection of an overdose of ketamine-medetomidine, and the carotid arteries were excised (each was bisected at both sides of the ligation site to obtain an approximately 3-mm segment). They were then stained with H&E, elastica van Gieson (EVG), or Masson's trichrome stain, or immunohistochemical (IHC) preparations in sequential sections as well, after fixation in 10% neutral-buffered formalin for 24 hours.[15,17,18] Analyses were performed in the ligated left common carotid arteries in all experiments, whereas the contralateral nonligated right carotid arteries served as a control.

The carotid arteries embedded in paraffin for histological examination were cut systematically in sequential sections (4 μm thick) by using a sliding microtome (Leica SM2010R; Leica Microsystems, Wetzler, Germany). The specimens of carotid artery were thoroughly examined by preparing sequential 500- to 750-μm cross sections for H&E or IHC stainings. A robust and reproducible vascular remodeling in WT mice reliably started at a distance of 500 μm from the ligature; small amounts of thrombus were observed at the ligation site,[3] and persisted up to 1500 μm from the ligature. Of each 20 sequential sections (one set), one was stained with H&E staining at least (ie, 80 μm thick intervals).[15,17,18] Quantifying analyses were performed in these 15 serial H&E sections collected from segments of approximately 500 to 1500 μm proximal to the site of ligation, as shown in Supplemental Figure S1. Images of the 15 sections were captured, and the thickened neointimal or medial areas and the intima/media (I/M) ratio were evaluated by a NanoZoomer Digital Pathology Virtual Slide Viewer (Hamamatsu Photonics Corp, Hamamatsu, Japan). The EVG staining clearly revealed both internal and external elastic lamina (EEL). In addition, the extent of constrictive vascular remodeling (reduction in vascular cross-sectional area) was calculated by the reduction in the EEL length in the ligated compared with the control artery (Hamamatsu Photonics Corp).[17,18] These indices were quantified by averaging all measurements counted in an individual mouse; we then selected one representative (mean) section per mouse.[15,17,18] To calculate proportions of collagen content to neointima, we measured intimal lesion areas and Masson's trichrome–positive blue areas in at least three sequential sections of each previously mentioned set, including the representative one, as previously described.[15,18]

The Ethics Committee of Animal Care and Experimentation, University of Occupational and Environmental Health (Kitakyushu, Japan) approved the protocols. They were performed according to the Institutional Guidelines for

Animal Experiments and the Law (number 105) and Notification (number 6) of the Japanese government. The investigation conforms to the Guide for the Care and Use of Laboratory Animals, published by the US NIH (publication 85-23, revised 1996).

Bone Marrow Transplantation

Bone marrow specimens (5×10^6 cells) obtained from the femurs of the desired donor mice (WT or *ASK1*$^{-/-}$) were transplanted into whole body–irradiated (9 Gy from a cesium γ source) recipients (8-week-old male WT mice), as previously described.[15,18,19] Carotid artery ligation was performed 5 weeks after the bone marrow transplantation (BMT); arteries were processed 4 weeks after the operation.

Immunohistochemistry

More than 10 animals from each group were analyzed. One representative section per mouse was prepared for IHC staining. Images from at least three sequential sections of each previously described 20 serial set (ie, 80 μm thick intervals), including the representative one, were captured and evaluated by a NanoZoomer Digital Pathology Virtual Slide Viewer to avoid potential bias.[15,17–19]

To detect the number of macrophages and SMCs in neointimal lesions, we used rat anti-mouse Mac-2 monoclonal antibody (1:500; Cedarlane Laboratories Ltd, Burlington, ON, Canada) for macrophages and monoclonal mouse anti-human smooth muscle actin (α-SMA) antibody (1:150; Dako Cytomation Co, Tokyo) for SMCs. For the latter, we applied the HistoMouse–*Plus* Kit (Invitrogen Corporation, Camarillo, CA) to block the endogenous mouse IgG. For evaluation of T-lymphocyte infiltration, especially in the neointimal lesions, a polyclonal rabbit anti-human CD3 antibody (1:1; Dako Cytomation Co) was used; we counted CD3$^+$ T cells.[18] To count neointimal microvessels, we used rat monoclonal antibody against mouse CD31 (1:20; Dianova, Hamburg, Germany).

To analyze apoptotic or proliferative activity of infiltrating cells in neointimal lesions, Bax rabbit polyclonal antibody (1:50; Santa Cruz Biotechnology, Inc., Santa Cruz, CA) or Ki-67 (MIB-1; 1:2000; Epitomics, Burlingame, CA) rabbit monoclonal antibody was applied, respectively. To evaluate ASK1 in injured carotid arteries, we used rabbit anti-ASK1 polyclonal antibody (1:50; Santa Cruz Biotechnology, Inc.).[15]

BrdU and TUNEL Staining

To label proliferating cells in the intimal lesion of ligated arteries 2 weeks after ligation, 50 mg/kg body weight 5′-bromo-2′-deoxyuridine (BrdU; Sigma-Aldrich, St. Louis, MO) was s.c. injected 2 hours before sacrifice; BrdU-incorporated cells were detected by IHC using a monoclonal mouse anti-BrdU antibody (Roche Applied Science, Lewes, UK). To detect the number of apoptotic cells *in vivo* (2 weeks after ligation) and *in vitro*, TUNEL assays were performed using an *In Situ* Cell Death Detection Kit (Roche Applied Science, Mannheim, Germany).[15]

The ligated arteries at 2 weeks were labeled with TUNEL reaction mixture (Roche Applied Science) and monoclonal mouse α-SMA antibody (1:1000; Dako Cytomation Co), and visualized with anti-fluorescein antibodies (TUNEL POD; Roche Applied Science) or goat anti-mouse IgG antibodies conjugated with Alexa Fluor Dyes (Invitrogen, Carlsbad, CA), respectively.[18] We also applied the HistoMouse *Plus* Kit (Invitrogen) to block the endogenous mouse IgG.

En Face Double-Immunofluorescence Staining

En face–prepared arteries in *ASK1*$^{-/-}$ and WT mice were fixed with cold acetone for 10 minutes and air dried for another 10 minutes, after being opened longitudinally with careful removal of luminal blood cells and adventitial adipose tissue, 1 week after ligation. *En face* vessels were labeled with TUNEL reaction mixture (Roche Applied Science) and rat monoclonal antibodies against mouse CD31 (1:20; Dianova), incubated with Hoechst 33258 (0.5 μg/mL; Dojindo, Kumamoto, Japan), and visualized with anti-fluorescein antibodies (TUNEL POD; Roche Applied Science) or goat anti-rat IgG and IgM antibodies conjugated with Alexa Fluor Dyes (Invitrogen), respectively. Stained tissues were placed on a glass slide, intimal side up, coverslipped by surface tension, and then viewed by confocal laser scanning microscopy (LSM5 Pascal Exciter; Carl Zeiss, Oberkochen, Germany) with ×40 UPlanApo oil immersion objectives. Three to six representative high-power fields (approximately 100 cells) were counted for numbers of TUNEL$^+$, CD31$^+$, Hoechst$^+$, and CD31$^+$ cells,[15,18] thereby expressing the number of apoptotic ECs as a percentage of total cells. We performed three experiments per group of animals, independently.

RT-PCR and Quantitative Real-Time RT-PCR

Total RNAs were extracted with TRIzol reagents (Invitrogen) from left carotid arteries of mice sacrificed at 3 weeks after ligation injury, at an approximate distance of 500 to 1500 μm from the ligature, after careful removal of luminal blood cells and adventitial adipose tissue, using the contralateral nonligated right carotid arteries as controls.

All procedures were performed as previously described.[15,17–19] RNase-free conditions were used to prevent mRNA degradation. First-strand cDNA was synthesized with Superscript II RT (Invitrogen) using random primers, according to the manufacturer's instructions. Quantitative real-time RT-PCR was performed using the TaqMan fluorogenic probe method with an ABI PRISM 7000 PCR machine (Perkin-Elmer Applied Biosystems, Foster, CA). Sequences of specific primers for RT-PCR are summarized in Table 1. Cycling conditions were as follows: 50°C for 2 minutes, 95°C for 10 minutes, followed by 45 cycles of

Table 1 Primers and Probes Used for Real-Time PCR

Oligo	Sequence
ASK1	
Forward	5′-ACGACCACCTCAGGGTCATTC-3′
Reverse	5′-TGGTCAGTTTCACAAAGTGTTTATATATCAG-3′
Probe	5′-AGACTGAAGACACCAGCGTGGTACCTCAAGT-3′
Bak	
Forward	5′-CTGGAACCCAACAGCATCTTG-3′
Reverse	5′-TGGTGAAGAGTTCGTAGGCATTC-3′
Probe	5′-CGGAGATGATATTAACCGGCGCTACGAC-3′
Bax	
Forward	5′-ATGGGCTGGACACTGGACTTC-3′
Reverse	5′-GAGGACTCCAGCCACAAAGATG-3′
Probe	5′-TGGCTGGGAAGGCCTCCTCTCCTACT-3′
CD54	
Forward	5′-CAAACAGGAGATGAATGGTACATACG-3′
Reverse	5′-ACCAGAATGATTATAGTCCAGTTATTTTGAG-3′
Probe	5′-CCATGGGAATGTCACCAGGAATGTGTACC-3′
CD106	
Forward	5′-CTCATTCCCTGAAGATCCAGTAATTAA-3′
Reverse	5′-TCAAAGGGATACACATTAGGGACTGT-3′
Probe	5′-TGAGTGGGCCACTTGTGCATGGG-3′
iNOS	
Forward	5′-GCAGTGGAGAGATTTTGCATGAC-3′
Reverse	5′-ATGGACCCCAAGCAAGACTTG-3′
Probe	5′-CACCACAAGGCCACATCGGATTTCAC-3′
IL-1β	
Forward	5′-TGCACTACAGGCTCCGAGATG-3′
Reverse	5′-GTACAAAGCTCATGGAGAATATCACTTG-3′
Probe	5′-TGTCGGACCCATATGAGCTGAAAGCTCTC-3′
IL-6	
Forward	5′-TTACACATGTTCTCTGGGAAATCG-3′
Reverse	5′-TTGGTAGCATCCATCATTTCTTTG-3′
Probe	5′-TGAGAAAAGAGTTGTGCAATGGCAATTCTGAT-3′
NF-κB	
Forward	5′-CTGACCCCTGTCCTCTCACATC-3′
Reverse	5′-CCGGTTTACTCGGCAGATCTT-3′
Probe	5′-TGATAACCGGGCCCCCAACACTG-3′
PDGF-BB	
Forward	5′-ACCTCGCCTGCAAGTGTGA-3′
Reverse	5′-CTCGCTGCTCCCTGGATGT-3′
Probe	5′-AGTGACCCCTCGGCCTGTGACTAGAAGTC-3′
TNF-α	
Forward	5′-CCCAGACCCTCACACTCAGATC-3′
Reverse	5′-TGCTCCTCCACTTGGTGGTT-3′
Probe	5′-ATTCGAGTGACAAGCCTGTAGCCCACG-3′

An 18s ribosomal RNA TaqMan Ribosomal RNA Control Reagents VIC Probe was used (catalogue no. 430829; Applied Biosystems).

95°C for 15 seconds and 60°C for 1 minute. The C_T values were measured corresponding to the cycle number at which the fluorescent emission, monitored in real time, reached a threshold of 10 SDs greater than the mean baseline from cycles 1 through 15. Serial 1:10 dilutions of plasmid DNA, containing each target cDNA, were analyzed, and served as standard curves from which we determined the rate of change of C_T values. Copy numbers of target cDNA were estimated by standard curves. All reactions for samples were performed in triplicate. Data were averaged from values obtained in each reaction. To determine mRNA levels of various genes, an mRNA expression index was used, which is an mRNA expression level standardized by 18S ribosomal RNA. The mRNA expression index was calculated as follows, in arbitrary units: mRNA expression index = (copy numbers of target gene mRNA/copy numbers of 18S ribosomal RNA) × 1 Arbitrary Unit.

Preparation of Aortic SMCs and Analysis of ASK1 Expression or Stress-Induced Apoptosis in Cultured SMCs

Aortic SMCs from 4- to 6-week-old male mice, fed a normal chow diet, were isolated after treatment with collagenase type II solution (Gibco, Grand Island, NY) for 45 minutes at 37°C incubation; the inside lumen was flushed to remove ECs.[18] Aortas were cut lengthwise into square pieces (approximately 1 to 2 mm each), placed onto two-well glass slides in an incubator, and cultured in Dulbecco's modified Eagle's medium with 10% fetal bovine serum for >3 days. For ASK1 staining, SMCs were fixed in 95% acetone for 30 seconds at room temperature, permeabilized in 0.1% Triton X-100 for 2 minutes at 4°C, and then stained with a rabbit anti-ASK1 polyclonal antibody (1:50; Santa Cruz Biotechnology, Inc.) for 1 hour, washed with PBS, and reacted with anti-rabbit Ig conjugated with fluorescein isothiocyanate (Invitrogen, Life Technologies Japan Ltd, Tokyo) for fluorescence staining. Cells were then observed and images were captured immediately with a Nikon ECLIPSE E600 (Nikon, Tokyo, Japan) inverted fluorescence microscope.

For TUNEL staining, aortic SMCs isolated from WT and *ASK1*$^{-/-}$ mice were incubated for 17 hours with medium alone as a control or with medium containing TNF-α (100 ng/mL; Sigma), as previously described.[15,18] These SMCs were fixed in 95% acetone for 30 seconds at room temperature and permeabilized in 0.1% Triton X-100 for 2 minutes at 4°C, and then stained with a TUNEL reaction mixture (Roche Applied Science) for 30 minutes at room temperature and incubated with Hoechst 33258 (0.5 μg/mL; Dojindo) and propidium iodide (PI; 5 μg/mL; Sigma) for fluorescence double staining. Cells were then observed and images were captured immediately with a Nikon ECLIPSE E600 inverted fluorescence microscope. Three to six representative fields (approximately 100 cells) were counted for the numbers of TUNEL$^+$ cells, PI$^+$ cells, and total cells. Thereby, the number of apoptotic macrophages was expressed as a percentage of the total number of cells. We performed more than three experiments, independently.

Western Blot Analysis

Proteins (100 μg) isolated from WT and *ASK1*$^{-/-}$ mice ligated arteries were separated by electrophoresis on 10% SDS-PAGE gels and transferred onto polyvinylidene difluoride membranes (Bio-Rad Laboratories, Tokyo, Japan).

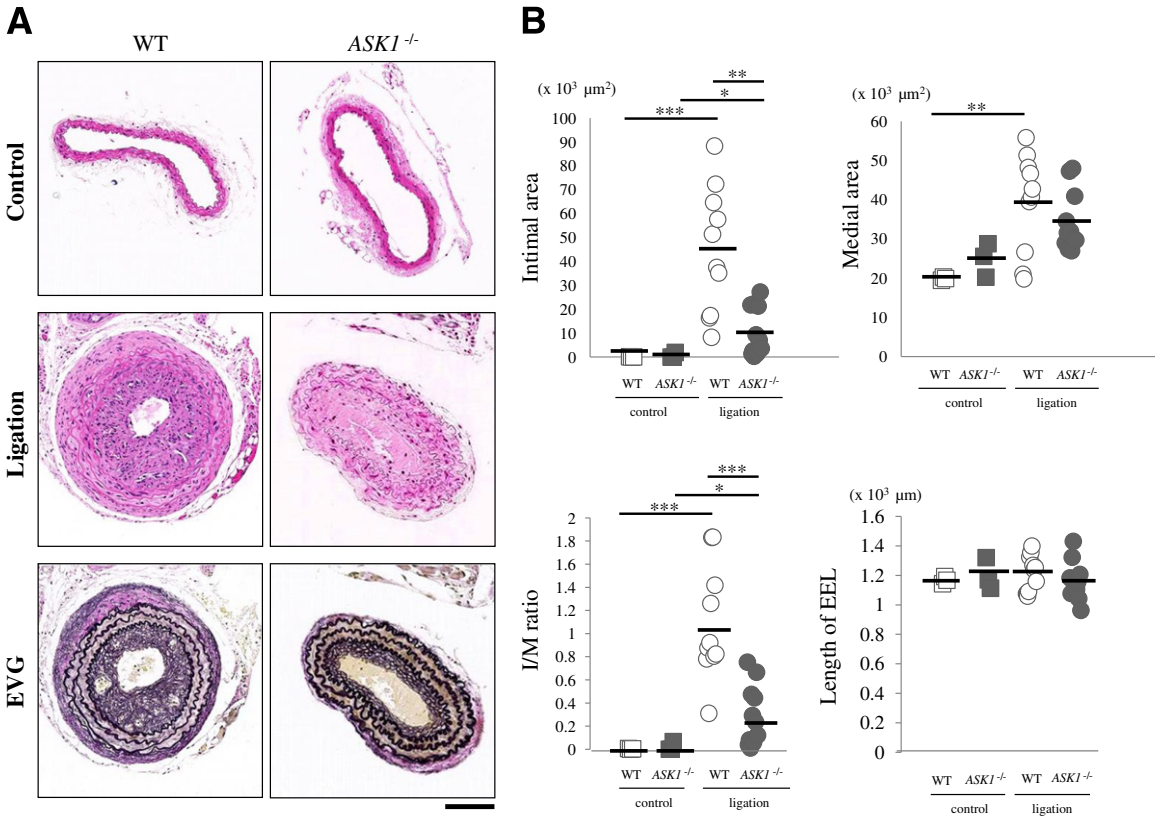

Figure 1 Histological analysis of ligation injury—induced remodeling arteries in non-BMT mice. **A**: Representative sequential sections of WT and *ASK1*$^{-/-}$ mice 3 weeks after ligation of the left common carotid arteries. The contralateral nonligated right carotid arteries serve as a control. EVG staining clearly reveals both internal elastic lamina (IEL) and EEL. **B**: Quantitative analysis demonstrates that the *ASK1*$^{-/-}$ mice significantly suppressed neointimal lesions compared with the WT mice, but not thickened medial ones. Thus, the I/M ratio of *ASK1*$^{-/-}$ mice is more markedly decreased than that of WT mice. However, EEL length is not significantly (N.S.) different between the two groups of mice. On the other hand, control arteries from both mice show few intimal areas and a low I/M ratio, along with a similar EEL length to the ligated arteries. Scale bar = 100 μm. $*P < 0.05$, $**P < 0.001$, and $***P < 0.0001$.

Membranes were incubated with mouse monoclonal antibodies to phosphorylated (phospho)-p38 (1:200; Santa Cruz Biotechnology, Inc.) or rabbit polyclonal antibody to Bax (1:50; Santa Cruz Biotechnology, Inc.) for the arteries.

ELISA for PDGF-BB

Levels of serum platelet-derived growth factor (PDGF)-BB in the ligation-injury model were measured using an enzyme-linked immunosorbent assay (ELISA) kit, according to the manufacturer's instructions (R&D Systems, Minneapolis, MN).[18]

Electron Microscopy

After 3 weeks, injured carotid arteries from *ASK1*$^{-/-}$ and WT mice were fixed with 2.5% glutaraldehyde, and small cut specimens (approximately 1 × 1 mm) of thickened neointima were immersed in 2% osmium tetroxide and dehydrated in ethanol. For transmission electron microscopy, the dehydrated tissue specimens were embedded in epoxy resin. Silver-gold sections produced with a diamond knife were transferred to copper grids and stained with uranyl acetate for viewing on a transmission electron microscope (JEM-1200EX; JEOL Ltd, Tokyo).

Statistical Analysis

Results are expressed as mean ± SE. Statistical significance was analyzed using the Student's *t*-test or *U*-test analysis, where appropriate. $P < 0.05$ was considered to be statistically significant.

Results

Expression of ASK1 under Basal Conditions and in Ligated Arteries from Non-BMT Vascular Remodeling Mice

Aortic SMCs isolated and harvested from WT mice specifically expressed ASK1, but not those from *ASK1*$^{-/-}$ mice, as detected by immunofluorescence (Supplemental Figure S2A). Real-time RT-PCR showed ligated and control arteries from WT mice to markedly express ASK1, compared with those from *ASK1*$^{-/-}$ mice ($P < 0.0001$ and $P < 0.05$, respectively) (Supplemental Figure S2B).

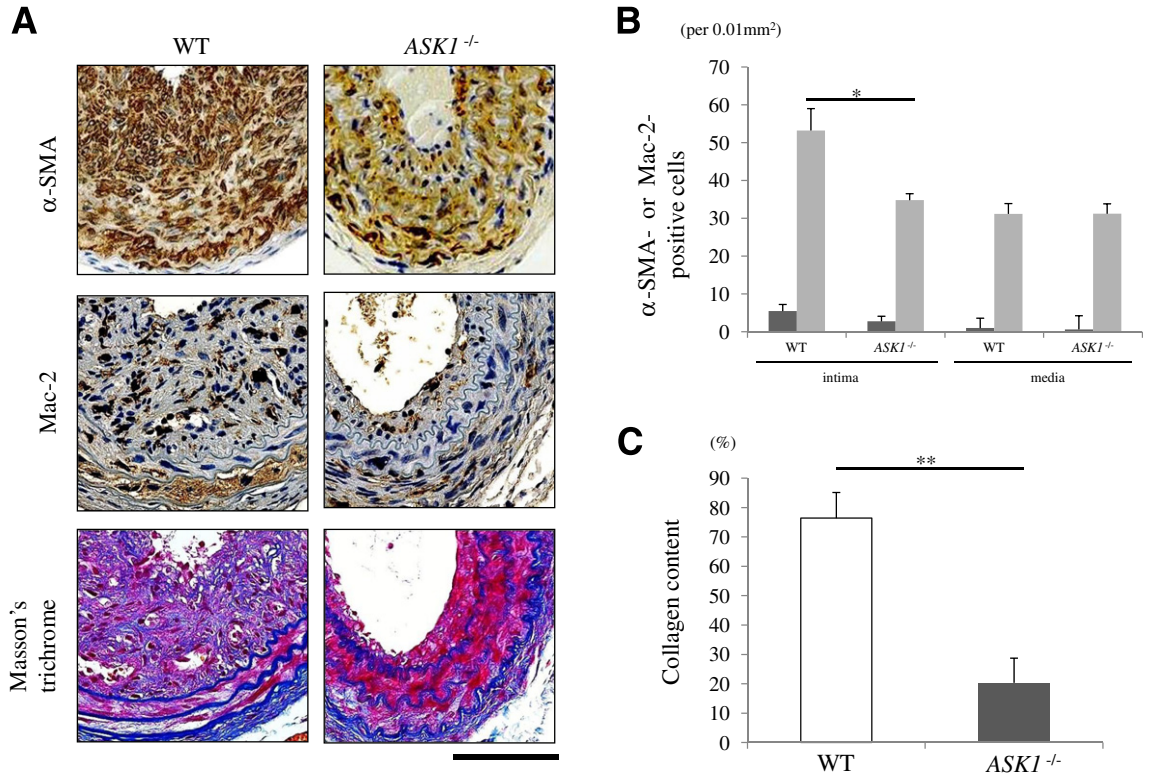

Figure 2 IHC and Masson's trichrome analyses of ligation injury—induced remodeling arteries in non-BMT mice. **A:** Representative IHC sequential sections of WT and *ASK1*$^{-/-}$ mice 3 weeks after ligation of the common carotid arteries. **B:** IHC shows that the numbers of intimal α-SMA^{+} SMCs (light grey bars) and Mac-2^{+} macrophages (dark grey bars) are significantly smaller in the neointimal lesions of *ASK1*$^{-/-}$ mice than those in the WT mice. By contrast, the proportion of neointimal SMCs in *ASK1*$^{-/-}$ mice is more significantly predominant than in the WT mice, whereas the numbers of medial SMCs and macrophages demonstrate no significant (N.S.) differences between the two groups of mice. **C:** There are larger amounts of collagen deposits in the neointimal hyperplasia of *ASK1*$^{-/-}$ mice than those in the WT mice. Scale bar = 100 μm. *$P < 0.05$, **$P < 0.001$.

Histological Evaluation of Ligated Arteries from Non-BMT Vascular Remodeling Mice

Quantitative analysis on sequential sections of common carotid arteries showed that *ASK1*$^{-/-}$ mice had significantly suppressed neointimal lesions compared with control WT mice after ligation-induced vascular remodeling for 3 weeks ($10.8 \pm 3.1 \times 10^3$ μm^2 versus $44.9 \pm 7.6 \times 10^3$ μm^2; $P < 0.001$), but not thickened medial areas ($34.3 \pm 2.3 \times 10^3$ μm^2 versus $39.2 \pm 4.0 \times 10^3$ μm^2; $P = 0.09$) (Figure 1A). Correspondingly, the I/M ratio of *ASK1*$^{-/-}$ mice was markedly decreased compared with WT mice (0.29 ± 0.08 versus 1.09 ± 0.16; $P < 0.0001$). However, EEL length was not significantly different between the two groups of mice (1093 ± 38 μm versus 1161 ± 39 μm for WT versus *ASK1*$^{-/-}$; $P = 0.27$). However, control arteries from both mice had few intimal areas and a low I/M ratio, with EEL length similar to the ligated arteries [intima, 66.7 ± 38.5 μm^2 versus 64.1 ± 46.1 μm^2 for WT versus *ASK1*$^{-/-}$ ($P = 0.23$); media, $19.9 \pm 0.2 \times 10^3$ μm^2 versus $22.9 \pm 1.5 \times 10^3$ μm^2 for WT versus *ASK1*$^{-/-}$ ($P = 0.09$); and EEL, 1167 ± 14 μm versus 1201 ± 62 μm for WT versus *ASK1*$^{-/-}$ ($P = 0.10$)]. Therefore, both types of mice showed little constrictive vascular remodeling.

IHC and Masson's Trichrome Analyses of Ligated Arteries in Non-BMT Vascular Remodeling Mice

IHC demonstrated that the α-SMA^{+} SMCs were fewer (34.8 ± 1.7 per 0.01 mm^2) in neointimal lesions of *ASK1*$^{-/-}$ mice, compared with those in the WT mice, 3 weeks after ligation-induced vascular remodeling (53.2 ± 5.8 per 0.01 mm^2; $P < 0.05$) (Figure 2, A and B). The number of neointimal Mac-2^{+} macrophages (Figure 2, A and B) showed a similar (borderline significant) difference to that of the neointimal SMCs between the two groups of mice (5.4 ± 1.8 versus 2.7 ± 1.4 per 0.01 mm^2 for WT versus *ASK1*$^{-/-}$; $P = 0.068$). However, the proportion of cell types in *ASK1*$^{-/-}$ mice (Mac-2^{+} cells: α-SMA^{+} cells = 6.9: 93.1% ± 3.5%) did not significantly differ from that in WT mice (ie, 9.39: 90.6% ± 2.8%; $P = 0.30$). By contrast, the medial SMCs and macrophages demonstrated no significant differences between the two groups of mice [SMCs, 31.2 ± 2.7 versus 31.2 ± 2.6 per 0.01 mm^2 for WT versus *ASK1*$^{-/-}$ mice ($P = 0.50$); macrophages, 0.95 ± 0.23 versus 0.60 ± 0.24 per 0.01 mm^2 for WT versus *ASK1*$^{-/-}$ mice ($P = 0.15$)].

As shown in Figure 2C, Masson's trichrome staining revealed that smaller amounts of collagen deposits were

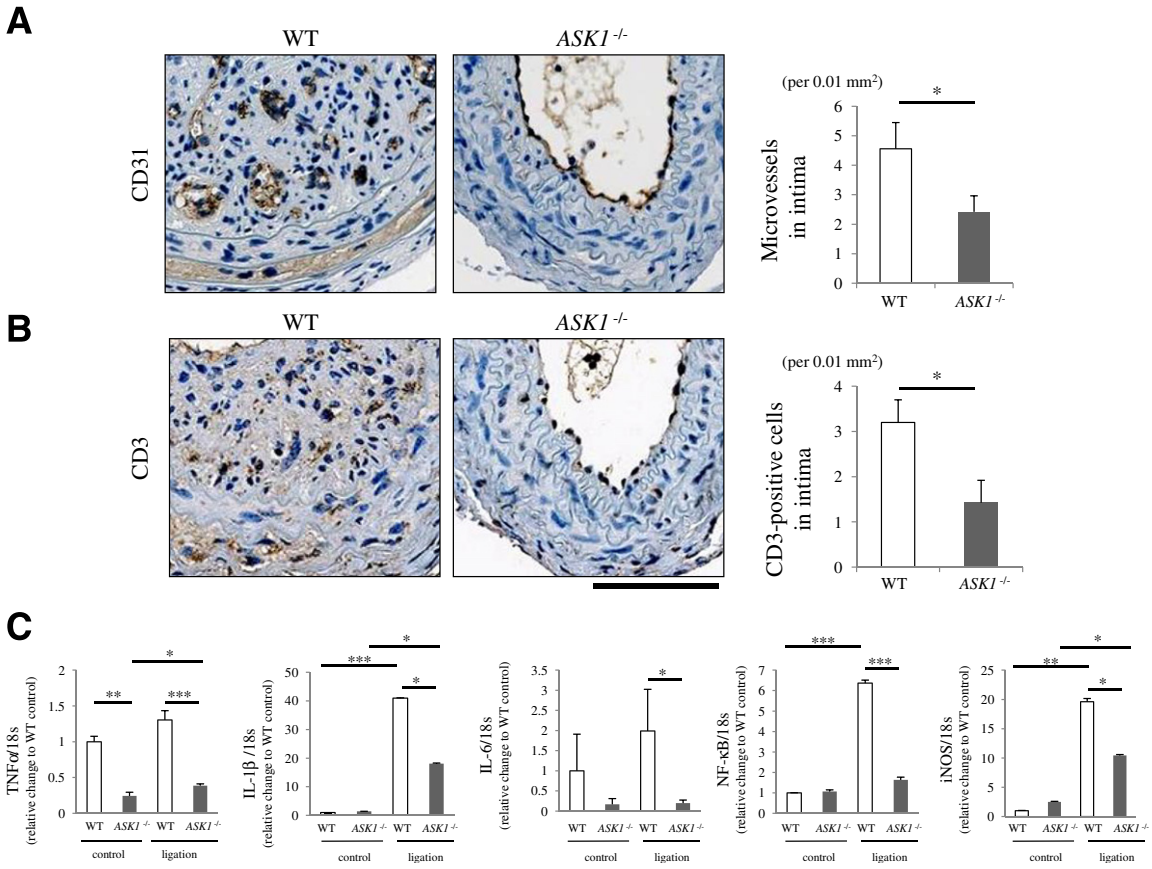

Figure 3 Analyses of IHC staining and gene expression of inflammatory signaling factors in ligation injury—induced remodeling arteries of non-BMT mice. **A**: IHC reveals that the number of $CD31^+$ neointimal microvessels is significantly lower in the ligated arteries of $ASK1^{-/-}$ mice than in that of the WT mice. **B**: Similarly, the number of $CD3^+$ infiltrating T lymphocytes in the neointimal lesions of $ASK1^{-/-}$ mice is significantly lower than that in the WT mice. **C**: Real-time RT-PCR shows that the expression levels of TNF-α, IL-1β, NF-κB1a, and inducible nitric oxide synthetase (iNOS) are significantly down-regulated in the $ASK1^{-/-}$ mice, compared with those in the WT and control mice. Scale bar = 100 μm. $^*P < 0.05$, $^{**}P < 0.001$, and $^{***}P < 0.0001$.

detected in neointimal lesions in the ligated arteries of $ASK1^{-/-}$ mice compared with those of WT mice (20.3% ± 8.7% versus 76.4% ± 8.4%; $P < 0.001$).

IHC staining also showed that the number of $CD31^+$ neointimal microvessels was significantly lower in the ligated arteries of $ASK1^{-/-}$ mice than in those of WT mice (2.42 ± 0.54 versus 4.56 ± 0.89 per 0.01 mm^2; $P < 0.05$) (Figure 3A). Taken together, the number of $CD3^+$ neointimal T cells was significantly decreased in the $ASK1^{-/-}$ mice than that in the WT mice (1.42 ± 0.50 versus 3.20 ± 0.50; $P < 0.05$) (Figure 3B).

Analysis of Gene Expression of Inflammatory Signaling Factors in Ligated Arteries of Non-BMT Vascular Remodeling Mice

Real-time RT-PCR showed that the expression levels of TNF-α, IL-1β, IL-6, NF-κB1a, and inducible nitric oxide synthase were significantly down-regulated in the ligated arteries of $ASK1^{-/-}$ mice, compared with those in WT and control mice ($P < 0.05$ or $P < 0.0001$, respectively) (Figure 3C).

Analysis of Expression of Phospho-p38 in Ligated Arteries of Non-BMT Vascular Remodeling Mice

Western blot analysis revealed significantly decreased expression of phospho-c-Jun N-terminal kinase and phospho-p38 in injured carotid arteries in $ASK1^{-/-}$ mice 3 weeks after ligation, compared with that in the WT mice (Supplemental Figure S2C).

Ultrastructural Analysis of Thickened Neointima in Ligated Arteries of Non-BMT Vascular Remodeling Mice

Electron microscopy was performed to determine *ASK1*-deficient SMC phenotypes in the neointima of ligated arteries on $ASK1^{-/-}$ mice, demonstrating that the phenotypes of intimal SMCs were predominantly contractile ones containing many bundles of thick and thin myofilaments (Supplemental Figure S3). By contrast, the SMC phenotypes of thickened neointima in the ligated WT arteries as a control mainly showed synthetic SMCs containing large amounts of rough endoplasmic reticulum or mitochondria (Supplemental Figure S3).

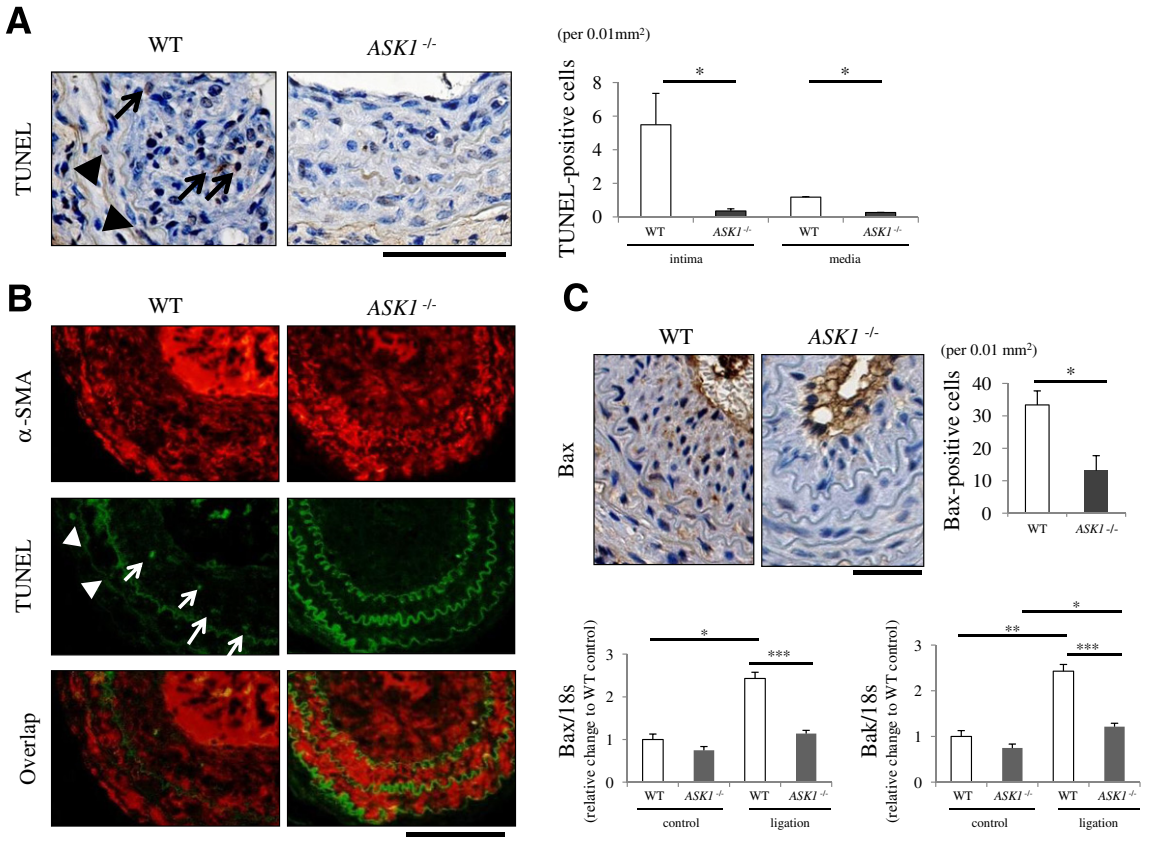

Figure 4 Analysis of apoptotic activity in ligation injury—induced remodeling arteries of non-BMT mice. **A:** The numbers of both TUNEL$^+$ neointimal and medial cells are significantly reduced in the *ASK1*$^{-/-}$ mice compared with the WT mice. **B:** Double-immunofluorescence staining confirms that these neointimal (**arrows**) and medial (**arrowheads**) apoptotic cells (TUNEL$^+$, green) are SMCs (α-SMA$^+$, red). **C:** The number of pro-apoptotic Bax$^+$ cells is significantly smaller in the neointima of *ASK1*$^{-/-}$ mice than that in the WT mice. Correspondingly, real-time RT-PCR shows greater decreases in expression of Bax and Bak in the ligated arteries of *ASK1*$^{-/-}$ mice than in the WT and control mice. Scale bar = 100 μm. *$P < 0.05$, **$P < 0.001$, and ***$P < 0.0001$.

Analysis of Apoptotic Activity in Ligated Arteries of Non-BMT Vascular Remodeling Mice

Although a small, but substantial, number of apoptotic cells was observed in both groups of mice 2 weeks after the ligation, the number of TUNEL$^+$ neointimal cells was significantly lower in the *ASK1*$^{-/-}$ mice (0.4 ± 0.1 per 0.01 mm^2; $P < 0.05$) than in the WT mice (5.5 ± 1.9 per 0.01 mm^2) (Figure 4A). However, TUNEL$^+$ medial cells were different between the two groups (1.18 ± 0.03 versus 0.26 ± 0.01 per 0.01 mm^2 for WT versus *ASK1*$^{-/-}$ mice; $P < 0.0001$) (Figure 4A). Double-immunofluorescence staining (Figure 4B) confirmed that these neointimal and medial apoptotic cells were SMCs.

The number of Bax$^+$ cells in the neointimal areas was significantly reduced in the *ASK1*$^{-/-}$ mice (6.2 ± 1.9 per 0.01 mm^2) compared with the WT mice (16.2 ± 4.3 per 0.01 mm^2; $P < 0.05$) (Figure 4C). Correspondingly, real-time RT-PCR demonstrated that the expression of Bax and Bak was more significantly decreased in the ligated arteries of *ASK1*$^{-/-}$ mice than in the WT and control mice ($P < 0.0001$ and $P < 0.05$, respectively) (Figure 4C).

En Face Double Immunofluorescence in Ligated Arteries of Non-BMT Vascular Remodeling Mice

The percentage of TUNEL$^+$ and CD31$^+$ ECs was also significantly lower in *ASK1*$^{-/-}$ mice than in WT mice 1 week after the ligation (0.6% ± 0.2% versus 6.3% ± 1.1%; $P < 0.05$) (Figure 5A).

Analysis of Gene Expression of Adhesion Molecules in Ligated Arteries of Non-BMT Vascular Remodeling Mice

Real-time RT-PCR revealed that the expression levels of CD54 and CD106 were significantly down-regulated in the ligated arteries of *ASK1*$^{-/-}$ mice, compared with those in WT and control mice ($P < 0.0001$ and $P < 0.001$, respectively) (Figure 5B).

Analysis of Proliferating Activity in Ligated Arteries of Non-BMT Vascular Remodeling Mice

In analysis of proliferation activity, BrdU$^+$ or MIB-1$^+$ cells in thickened neointimal lesions 2 weeks after ligation were relatively few and showed no significant difference

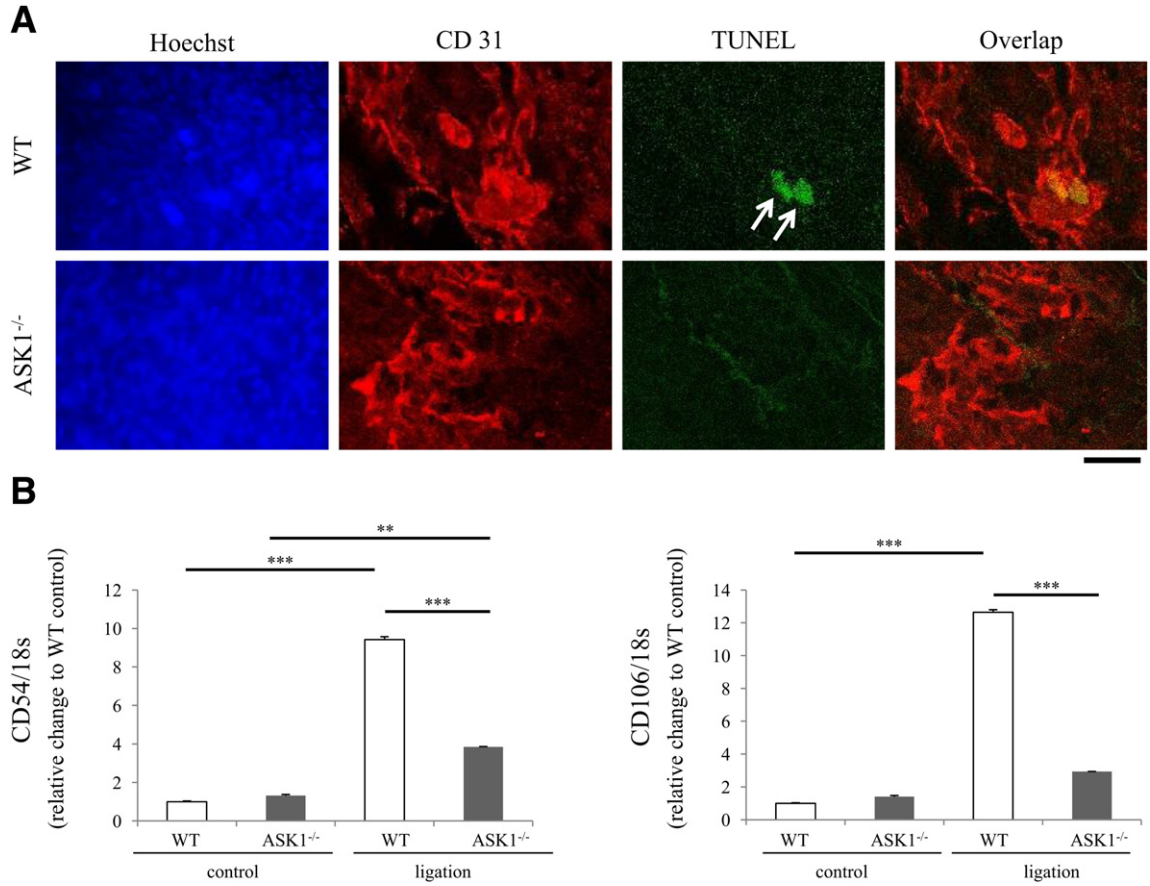

Figure 5 Analyses of *en face* double immunofluorescence and gene expression of adhesion molecules in ligation injury–induced remodeling arteries of non-BMT mice. **A:** Arterial ECs were analyzed by fluorescence double staining with TUNEL (green) and mouse CD31 (red), and confocal laser-scanning images were captured from the same field (*en face* images). The percentage of both TUNEL$^+$ and CD31$^+$ ECs (**arrows**) is significantly lower in those from *ASK1*$^{-/-}$ mice, compared with WT mice. Apoptotic cell counts from three to six representative high-power fields (approximately 100 cells) were performed, and expressed as percentages of apoptotic cells/total cells, stained with both TUNEL and CD31 (merged)/both Hoechst (blue) and CD31, respectively. Images are representative of three animals per group. Original magnification, ×400. Scale bar = 50 μm. **B:** Real-time RT-PCR shows that the expression levels of CD54 and CD106 are significantly down-regulated in the ligated arteries of *ASK1*$^{-/-}$ mice, compared with those in the WT and control mice. $^{**}P < 0.001$, $^{***}P < 0.0001$.

between the two groups of mice [BrdU, 2.0 ± 0.9 versus 2.2 ± 1.2 per 0.01 mm^2 for WT versus *ASK1*$^{-/-}$ mice ($P = 0.38$); MIB-1, 2.7 ± 0.9 versus 1.2 ± 0.9 per 0.01 mm^2 for WT versus *ASK1*$^{-/-}$ mice ($P = 0.13$)] (Figure 6A). Because the neointimal vascular cells showed low proliferation rates in our model, these data suggested that BrdU$^-$ and MIB-1$^-$ cells arise by migration, most likely from media.

Analysis of PDGF-BB Expression in Ligated Arteries of Non-BMT Vascular Remodeling Mice

The results of ELISA demonstrated that the serum PDGF-BB levels were significantly lower in *ASK1*$^{-/-}$ mice than in WT mice 3 weeks after the artery ligation (875.5 ± 70.5 versus 1172.2 ± 158.7 pg/mL; $P < 0.05$) (Figure 6B). Real-time RT-PCR also showed significantly lower expression of PDGF-BB in the ligated arteries of *ASK1*$^{-/-}$ mice than in WT and control mice ($P < 0.0001$ and $P < 0.05$, respectively) (Figure 6B).

TNF-α (Immune System)–Induced Apoptosis in Cultured Aortic SMCs

The nuclear morphological characteristics of SMCs were observed after double staining with PI and Hoechst 33258; TUNEL$^+$ apoptotic cells were analyzed in the same fields (Figure 7). Few apoptotic cells were detected in untreated macrophages. When the cells were incubated with TNF-α, the apoptotic SMC count was markedly increased. However, the apoptotic cell counts with TUNEL staining were significantly reduced in the *ASK1*$^{-/-}$ mice compared with WT mice in experimental conditions. *ASK1*$^{-/-}$ mice had significantly fewer TUNEL$^+$ cells compared with WT mice after they were treated with TNF-α (1.6% ± 0.8% versus 31.4% ± 7.3%; $P < 0.05$).

Histological and IHC Analysis of BMT Vascular Remodeling Mice

As with the non-BMT data, BMT mice from *ASK1*$^{-/-}$ donors significantly suppressed neointimal lesion areas

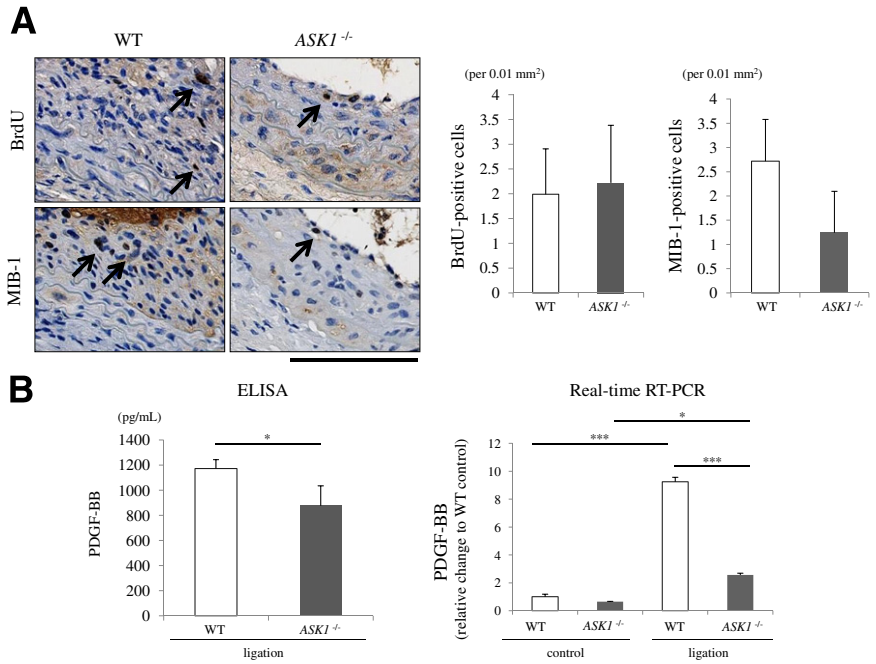

Figure 6 Analyses of proliferating activity and mPDGF-BB expression in ligation injury—induced remodeling arteries of non-BMT mice. **A:** The thickened neointimal lesions have relatively few BrdU$^+$ or MIB-1$^+$ cells, and show no significant differences between the two groups of mice. Because neointimal vascular cells have low proliferation rates in our model, this suggests that BrdU$^-$ or MIB-1$^-$ cells arise by migration, most likely from the media. **B:** ELISA results show that serum PDGF-BB levels are significantly lower in *ASK1*$^{-/-}$ mice than in WT mice. Real-time RT-PCR also shows significantly greater PDGF-BB expression in ligated arteries of *ASK1*$^{-/-}$ mice than in those of the WT and control mice. Scale bar = 100 μm. **P* < 0.05, ***P* < 0.001.

compared with WT donors [intima, 44.8 ± 9.0 × 10^3 μm^2 versus 11.8 ± 4.6 × 10^3 μm^2 for WT versus *ASK1*$^{-/-}$ donors ($P < 0.05$); media, 43.6 ± 3.1 × 10^3 μm^2 versus 26.5 ± 2.4 × 10^3 μm^2 for WT versus *ASK1*$^{-/-}$ donors ($P = 0.08$)] (Figure 8, A and B). Therefore, the I/M ratio of *ASK1*$^{-/-}$ donor BMT mice was greatly suppressed versus WT donors (0.37 ± 0.10 versus 1.14 ± 0.34; $P < 0.05$) (Figure 8B). In IHC analysis, the number of α-SMA$^+$ SMCs in neointimal lesions was not significantly different between the two mouse groups (158.6 ± 35.5 versus 92.8 ± 31.9 per 0.01 mm^2 for WT versus *ASK1*$^{-/-}$ donors; $P = 0.10$), whereas that of Mac-2$^+$ macrophages was significantly fewer in neointimal lesions of *ASK1*$^{-/-}$ donors, compared with the WT donors (25.2 ± 7.8 versus 66.2 ± 12.1 per 0.01 mm^2; $P < 0.05$; data not shown). In addition, these intimal SMCs were slightly positive for ASK1 in BMT mice from WT donors, but not from *ASK1*$^{-/-}$ donors (data not shown).

Discussion

The present study demonstrates a critical role of ASK1 in mechanical injury—induced vascular remodeling, because both (non-BMT) *ASK1*$^{-/-}$ mice and BMT-recipient WT mice from *ASK1*$^{-/-}$ donors have significantly suppressed ligation injury—induced neointimal hyperplasia that can

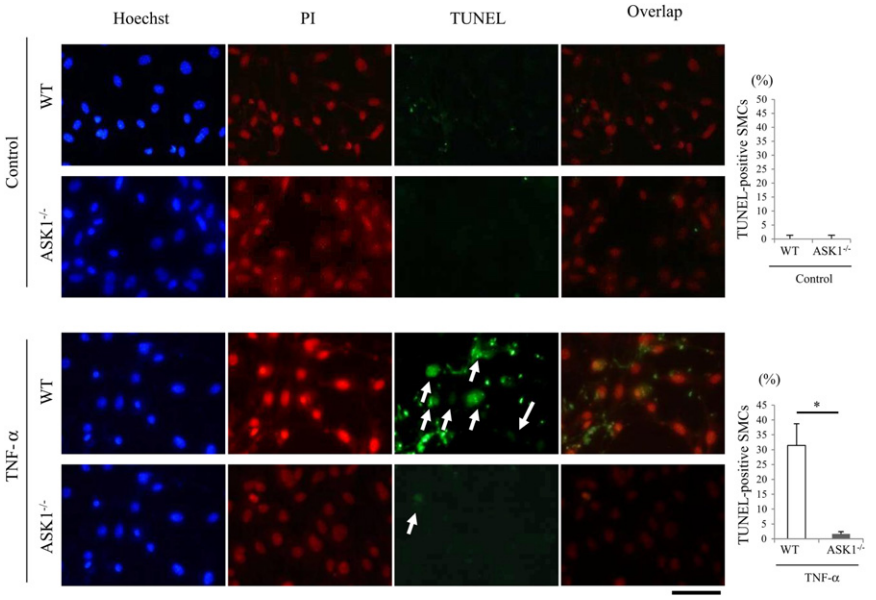

Figure 7 Immune system—induced apoptosis in cultured aortic SMCs. Aortic SMCs are analyzed by fluorescence double staining with PI (red-orange) and Hoechst 33258 (blue), and TUNEL$^+$ cells (green) are shown; images are captured from the same field. SMCs from WT or *ASK1*$^{-/-}$ mice are incubated with medium alone (Control) or medium containing 100 ng/mL TNF-α. Although few apoptotic SMCs are seen in the untreated control mice, the percentage of TUNEL$^+$ cells (**arrows**) is higher in SMCs from WT mice in the treatment, compared with *ASK1*$^{-/-}$ mice. Apoptotic cell counts from three to six representative fields (approximately 100 cells) for each condition are performed, and expressed as percentages of total cells stained with TUNEL or PI. Original magnification, × 200. Scale bar = 100 μm. **P* < 0.05.

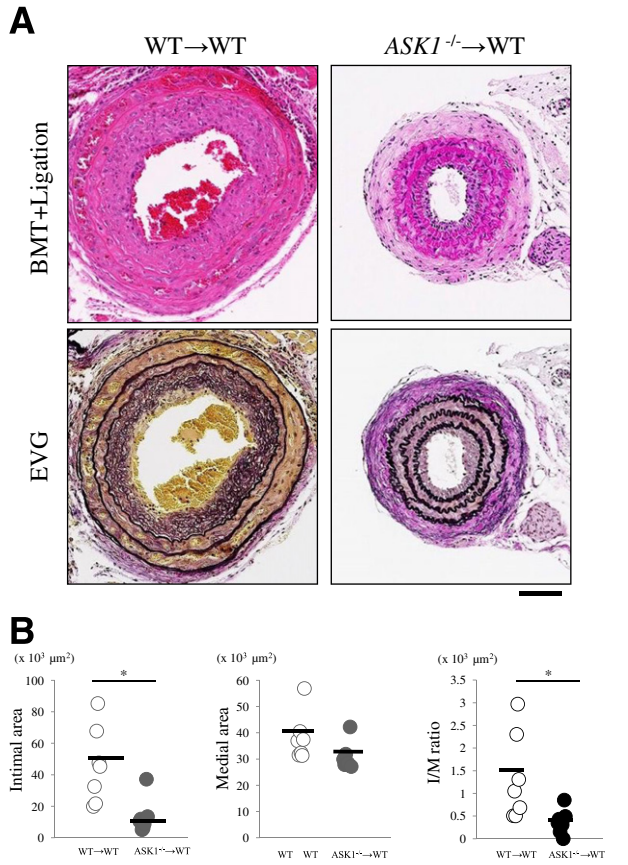

Figure 8 Histological analysis of ligation injury–induced remodeling arteries in BMT mice. **A**: Representative sequential sections of BMT mice from WT and *ASK1*$^{-/-}$ donors 4 weeks after ligation of the common carotid arteries. EVG staining clearly reveals both internal elastic lamina and EEL. **B**: Similar to the non-BMT data, quantitative analysis demonstrates that BMT mice from *ASK1*$^{-/-}$ donors significantly suppresses neointimal lesion areas compared with those from WT donors. Scale bar = 100 μm. *$P < 0.05$.

basically confirm the concepts, as previously reported by Izumi et al.[16] Compared with the WT mice, the *ASK1*$^{-/-}$ mice revealed potentially anti-atherosclerotic profiles, including manifestations of fewer SMC-predominant intimal lesions and fewer neointimal microvessels, associated with repression of apoptosis in SMCs and ECs. Although these characteristics apparently contradict our previous results of *ASK1* and *apoE* double-knockout mice on a hypercholesterolemia model,[15] atherosclerosis is an extremely complex disease, orchestrated by multiple factors, including disturbed blood flow, elevated inflammatory cytokines, apoptotic activity, and oxidative stress.[17,18,20] Indeed, the hyperlipidemia-induced mouse atherosclerotic model demonstrates the progression of macrophage-rich intimal lesions with necrotic lipid cores and fibrous cap formation, reminiscent of human atheromatous plaques, manifesting as chronic inflammatory disease.[15] In particular, inflammatory cells, especially macrophages, play crucial roles in the hypercholesterolemia-induced atherosclerosis via macrophage apoptosis per se.[15] However, the current model shows the SMC-rich neointimal hyperplasia without definite evidence of necrotic cores, likely reminiscent of human restenosis after angioplasty or shoulder lesions of vulnerable atheroma, manifesting as acute to subacute inflammatory disease. Similarly, SMCs, in particular, have pivotal roles in the ligation-induced atherosclerotic model via their own apoptotic activity. Thus, the mechanisms responsible for atherosclerosis must be fundamentally different between these two models, from the aspects of predominant cell types undergoing apoptosis, at the least.

The significantly fewer TUNEL^{+} SMCs were found in both the smaller neointima and media in *ASK1*$^{-/-}$ mice, and were associated with decreased Bax expression, compared with WT mice (Figure 4). Our *in vitro* examination confirmed this result, because immune system (TNF-α)–mediated apoptosis was markedly attenuated in cultured aortic SMCs obtained from *ASK1*$^{-/-}$ mice (Figure 7). These results are in agreement with the following observations of other groups: antioxidant therapy (using tempol) prevented neointimal formation, along with repressed apoptosis and migration of medial SMCs in balloon-injured rat carotid arteries by inhibiting pro-apoptotic Bax induction[21]; and vascular medial SMC apoptosis induced by diphtheria toxin increased both medial and neointimal areas, when apoptosis was augmented after ligation injury of mouse carotid arteries and during vascular remodeling.[22] Moreover, we show, for the first time to our knowledge, that reduced apoptosis by intimal SMCs can also suppress vascular remodeling. On the other hand, these neointimal SMCs in the *ASK1*$^{-/-}$ mice showed predominantly differentiated contractile phenotypes, containing many bundles of thin myofilaments, rather than dedifferentiated synthetic cells (Supplemental Figure S3), accompanied by significantly reduced collagen production (Figure 2). However, less synthesis of extracellular matrix in the *ASK1*$^{-/-}$ mice might partly result from efficient efferocytosis.[9,10] Hayashi et al[23] have shown that p38 mitogen-activated protein kinase, downstream of ASK1 signaling, plays a crucial role in SMC dedifferentiation when stimulated by PDGF-BB; and that the p38 mitogen-activated protein kinase pathway partially mediates phenotypes of vascular SMCs. The previously described data, under conditions of *ASK1* deficiency, reveal that p38 signals were significantly decreased in the ligated arteries (Supplemental Figure S2), and may be consistent with their suggestions. Because ASK1 is reportedly located in a critical upstream position for many signal transduction pathways, *ASK1* deficiency should suppress many signals required for cell survival, apoptosis, and differentiation.[15,24] Furthermore, the *en face* aortic double-immunofluorescence staining (Figure 5) indicated that the blockade of the ASK1/p38 signal can also protect CD31^{+} ECs against apoptosis. Apoptosis of endothelium must be important as well, because the initial step for injury-induced vascular remodeling or atherosclerosis includes endothelial damage, increased expression of adhesion molecules, and inflammatory cell migration.[11,18,20] In fact, we demonstrated that

numbers of intimal macrophages and T lymphocytes in the neointima of *ASK1*$^{-/-}$ mice were significantly decreased, and associated with down-regulated expression of several adhesion and pro-inflammatory genes, compared with those in WT mice (Figures 2, 3, and 5).

Among many pro-inflammatory cytokines or growth factors, PDGF expression differed significantly between the two groups of mice (Figure 6B). PDGF-BB, produced by platelets, macrophages, and vascular cells at sites of inflammation and damage in the arterial wall, is a strong activator of SMC migration or replication and one of the most important factors in atherogenesis.[11,18,25] Based on our data, considering that most intimal cells were BrdU^{-} or MIB-1^{-} cells (Figure 6A), stimulated PDGF secretion would significantly accelerate SMC migration, rather than proliferation,[22,26] into the more enhanced neointima of WT mice, and intimal SMC dedifferentiation,[23] compared with those in *ASK1*$^{-/-}$ mice. Thus, the ASK1 pathway might also have a close relationship with PDGF-induced migratory signaling in neointimal SMCs, although detailed molecular mechanisms are unclear. Intimal SMCs in the WT mice could have originated from ASK1-expressed medial SMCs, ASK1-expressed circulating SMC precursors, or adventitial SMC progenitors,[17–19] because ASK1 is ubiquitously expressed by multiple cell types in the vasculature.[15] We previously found that bone marrow–derived progenitor cell migration into the intima plays a critical role in initiation and progression of atherosclerosis in histamine-deficient mice, by showing recruitment of green fluorescent protein^{+} monocytes/macrophages and/or SMCs.[19] Similarly, the current BMT study using the *ASK1*$^{-/-}$ to WT mice (Figure 8) confirmed the results obtained from the non–BMT-*ASK1*$^{-/-}$ mice (Figure 1), in which the migrated *ASK1*-deficient SMCs alone might have a protective role against the ligation injury–induced vascular remodeling. Also, ASK1-deficient immune cells, including macrophages and T lymphocytes, may play some important roles in this BMT model, as well as *ASK1*-deficient SMCs, although to a lesser degree, because BMT replaces whole immune cells of recipient WT mice with those of donor *ASK1*$^{-/-}$ mice.

Microvessels within the intima of atherosclerotic plaques play important roles in the growth and progression of macrophage-rich vulnerable atheroma, associated with promotion of intraplaque hemorrhage.[27] By contrast, the effect of intimal neovascularization on vascular remodeling is not well described, although one study reported that the human coronary intimal microvessels definitely played a significant role in the growth of plaques by supplying both inflammatory cells and plasma components, such as albumin and fibrinogen.[28] We can support this suggestion and demonstrate, for the first time to our knowledge, that more neointimal microvessels occur in the more enhanced intimal lesions of WT mice, together with greater infiltration of T lymphocytes, macrophages, and SMCs, and up-regulated expression of various inflammatory signaling factors, compared with those of *ASK1*$^{-/-}$ mice (Figures 2, 3, and 5). Our data strongly confirm the hypothesis that intimal microvessels can promote ligation injury–induced vascular remodeling and might contribute to the evolution of atherosclerosis, by providing an extended surface area of activated ECs to hasten further recruitment of inflammatory cells and SMCs.[29] Furthermore, the newly formed vascular channels might be prone to rupture; subsequent thrombosis formation *in situ* can stimulate thrombin-mediated events, such as migration or proliferation of SMCs.[28] In this context, it is possible that ASK1 can alter the functional characteristics of ECs that influence monocyte adhesion, transmigration and activation of inflammatory cells or SMCs, and the apoptotic activity of ECs. Despite that, we cannot completely exclude the possibility that the significantly reduced neovascularization might partly result from decreased intimal size in *ASK1*$^{-/-}$ mice.

Therefore, our data suggest that *ASK1* deficiency plays critical roles in ameliorating neointimal progression, together with reduced migration of inflammatory cells or SMCs into the neointima via decreased neovascularization, as well as repressed apoptosis of ECs and/or both medial and intimal SMCs; and decreased synthesis of collagen-rich matrix, at least in part, via suppressed SMC dedifferentiation. A diagram depicting the crucial roles of ASK1 in the current model is summarized in Supplemental Figure S4. Thus, we can support the hypothesis that increased SMC apoptosis enhances the development of neointimal hyperplasia and exerts detrimental effects in injury-induced vascular remodeling. All these observations suggest that a specific ASK1 pathway blocker could offer a therapeutic strategy against atherosclerosis progression (eg, especially restenosis after angioplasty), by suppressing SMC migration and neovascularization. Furthermore, our obtained results indicate that ASK1 expression, especially in the SMCs, might be crucial and reciprocally responsible for various potentially pro-atherogenic effects, unlike our recent reports,[15] revealing that ASK1-expressed macrophages particularly played a significant anti-atherogenic role. We might confirm that the fundamental mechanisms responsible for atherosclerosis in these injured arteries are completely distinguished from those in the atheromatous plaques of aortas.

Supplemental Data

Supplemental material for this article can be found at *http://dx.doi.org/10.1016/j.ajpath.2012.10.008*.

References

1. Libby P, Schwartz D, Brogi E, Tanaka H, Clinton SK: A cascade model for restenosis: a special case of atherosclerosis progression. Circulation 1992, 86:III47–III52
2. Schwartz SM, deBlois D, O'Brien ER: The intima: soil for atherosclerosis and restenosis. Circ Res 1995, 77:445–465

3. Kumar A, Lindner V: Remodeling with neointima formation in the mouse carotid artery after cessation of blood flow. Arterioscler Thromb Vasc Biol 1997, 17:2238−2244
4. Libby P, Tanaka H: The molecular bases of restenosis. Prog Cardiovasc Dis 1997, 40:97−106
5. Cowan DB, Langille BL: Cellular and molecular biology of vascular remodeling. Curr Opin Lipidol 1996, 7:94−100
6. Ross R: Atherosclerosis: an inflammatory disease. N Engl J Med 1999, 340:115−126
7. Lusis AJ: Atherosclerosis. Nature 2000, 407:233−241
8. Malik N, Francis SE, Holt CM, Gunn J, Thomas GL, Shepherd L, Chamberlain J, Newman CM, Cumberland DC, Crossman DC: Apoptosis and cell proliferation after porcine coronary angioplasty. Circulation 1998, 98:1657−1665
9. Kockx MM, De Meyer GR, Muhring J, Jacob W, Bult H, Herman AG: Apoptosis and related proteins in different stages of human atherosclerotic plaques. Circulation 1998, 97:2307−2315
10. Flynn PD, Byrne CD, Baglin TP, Weissberg PL, Bennett MR: Thrombin generation by apoptotic vascular smooth muscle cells. Blood 1997, 89:4378−4384
11. Libby P: Inflammation in atherosclerosis. Nature 2002, 420:868−874
12. Kockx MM, Herman AG: Apoptosis in atherosclerosis: beneficial or detrimental? Cardiovasc Res 2000, 45:736−746
13. Ichijo H, Nishida E, Irie K, Digike PT, Saitoh M, Moriguchi T, Takagi M, Matsumoto K, Miyazono K, Gotoh Y: Induction of apoptosis by ASK1, mammalian MAPKKK that activates SAPK/JNK and p38 signaling pathways. Science 1997, 275:90−94
14. Tobiume K, Matsuzawa A, Takahashi T, Nishitoh H, Morita K, Takeda K, Minowa O, Miyazono K, Noda T, Ichijo H: ASK1 is required for sustained activations of JNK/p38 MAP kinases and apoptosis. EMBO Rep 2001, 2:222−228
15. Yamada S, Ding Y, Tanimoto A, Wang KY, Guo X, Li Z, Tasaki T, Nabesima A, Murata Y, Shimajiri S, Kohno K, Ichijo H, Sasaguri Y: Apoptosis signal-regulating kinase 1 deficiency accelerates hyperlipidemia-induced atheromatous plaques via suppression of macrophage apoptosis. Arterioscler Thromb Vasc Biol 2011, 31:1555−1564
16. Izumi Y, Kim S, Yoshiyama M, Izumiya Y, Yoshida K, Matsuzawa A, Koyama H, Nishizawa Y, Ichijo H, Yoshikawa J, Iwao H: Activation of apoptosis signal-regulating kinase 1 in injured artery and its critical role in neointimal hyperplasia. Circulation 2003, 108:2812−2818
17. Yamada S, Wang KY, Tanimoto A, Fan J, Shimajiri S, Kitajima S, Morimoto M, Tsutui M, Watanabe T, Yasumoto K, Sasaguri Y: Matrix metalloproteinase 12 accelerates the initiation of atherosclerosis and stimulates the progression of fatty streaks to fibrous plaques in transgenic rabbits. Am J Pathol 2008, 172:1419−1429
18. Guo X, Yamada S, Tanimoto A, Ding Y, Wang KY, Shimajiri S, Murata Y, Kimura S, Tasaki T, Nabeshima A, Watanabe T, Kohno K, Sasaguri Y: Overexpression of peroxiredoxin 4 attenuates atherosclerosis in apolipoprotein E knockout mice. Antioxid Redox Signal 2012, 17:1362−1375
19. Sasaguri Y, Wang KY, Tanimoto A, Tsutsui M, Ueno H, Murata Y, Kohno Y, Yamada S, Ohtsu H: Role of histamine produced by bone marrow-derived vascular cells in pathogenesis of atherosclerosis. Circ Res 2005, 96:974−981
20. Iuliano L: The oxidant stress hypothesis of atherogenesis. Lipids 2001, 36:41−44
21. Jagadeesha DK, Lindley TE, Deleon J, Sharma RV, Miller F, Bhalla RC: Tempol therapy attenuates medial smooth muscle cell apoptosis and neointima formation after balloon catheter injury in carotid artery of diabetic rats. Am J Physiol Heart Circ Physiol 2005, 289:H1047−H1053
22. Yu H, Clarke MCH, Figg N, Littlewood TD, Bennett MR: Smooth muscle cell apoptosis promotes vessel remodeling and repair via activation of cell migration, proliferation, and collagen synthesis. Arterioscler Thromb Vasc Biol 2011, 31:2402−2409
23. Hayashi K, Takahashi M, Kimura K, Nishida W, Saga H, Sobue K: Changes in the balance of phosphoinositide 3-kinase/protein kinase B (Akt) and the mitogen-activated protein kinases (ERK/p38 MAPK) determine a phenotype of visceral and vascular smooth muscle cells. J Cell Biol 1999, 145:727−740
24. Muniyappa H, Das KC: Activation of c-Jun N-terminal kinase (JNK) by widely used specific p38 MAPK inhibitors SB202190 and SB203580: a MLK-3-MKK7-dependent mechanism. Cell Signal 2008, 20:675−683
25. Thyberg J, Ostman A, Backstrom G, Westermark B, Heldin CH: Localization of platelet-derived growth factor (PDGF) in CHO cells transfected with PDGF A- and B-chain cDNA: retention of PDGF-BB in the endoplasmic reticulum and Golgi complex. J Cell Sci 1990, 97: 219−229
26. Clowes AW, Schwartz SM: Significance of quiescent smooth muscle migration in the injured rat carotid artery. Circ Res 1985, 56:139−145
27. Moulton KS, Heller E, Konerding MA, Flynn E, Palinski W, Folkman J: Angiogenesis inhibitors endostatin or TNP-470 reduce intimal neovascularization and plaque growth in apolipoproetin E-deficient mice. Circulation 1999, 99:1726−1732
28. Zhang Y, Cliff WJ, Schoefl GI, Higgins G: Immunohistochemical study of intimal microvessels in coronary atherosclerosis. Am J Pathol 1993, 143:164−172
29. Aikawa M, Libby P: The vulnerable atherosclerotic plaque pathogenesis and therapeutic approach. Cardiovasc Pathol 2004, 13:125−138